

PERFORMANCE ANALYSIS OF FEEDBACK CONTROLLED IRRIGATION CANALS USING FREQUENCY RESPONSE METHODS

Ömer Faruk DURDU¹

ABSTRACT

A feedback control strategy was used to regulate an irrigation canal to minimize the magnitude and duration of the mismatch between the supply and the demand of water. To derive the control system, the Saint-Venant equations of open-channel flow were linearized using Taylor series and a finite-difference approximation of the original nonlinear, partial differential equations around the initial steady state or equilibrium conditions. Using optimal control theory, a stochastic (Linear Quadratic Gaussian (LQG)) controller was designed to generate optimal gate opening and to estimate state vectors. Since state vectors (flow rate and depth) were estimated in the operation of the irrigation canal, LQG controller did not provide appropriate performance like other deterministic approaches (e.g. Linear Quadratic Regulator (LQR)) did. Therefore, LQG feedback controller for the irrigation canal was tuned by using a loop shaping technique to recover LQR performance capability before committing to implementation. To analyze the performance of LQG controlled irrigation canal, frequency response techniques (singular values (SV) and Bode diagram) were employed. Frequency response methods were found to be great techniques to analyze the performance of feedback controlled irrigation canals and to demonstrate the improvement in the performance of the control system when a loop shaping technique was employed.

Keywords: feedback control; irrigation canals; singular values; Bode diagram.

Geri Beslemeli Sistemle Kontrol Edilen Sulama Kanallarının Frekans Cevabı Yöntemleri ile Performans Analizi

ÖZET

Sulama suyu talep ve arz miktarları arasındaki dengesizliği zaman ve miktar açısından minimize etmek için geribeslemeli bir kontrol sistemi sulama kanalı regülasyonunda kullanılmıştır. Kontrol sisteminin oluşturulması için sulama kanallarındaki akımı ifade eden Saint-Venant eşitlikleri Taylor serileri ve sonlu-farklar tekniği kullanılarak doğrusal eşitlik haline getirilmiştir. Bu doğrusallaştırma denge halindeki akım şartları referans kabul edilerek yapılmış ve kapaktaki açılıp kapanmanın akım miktarına ve derinliğine olan etkisini anlatan bir çift adi türevsel denklem geliştirilmiştir. Optimum kapak açıklığını hesaplamak ve durum vektörlerini tahmin etmek için optimal kontrol teorisi kullanılarak stokastik bir kontrol mekanizması (doğrusal karesel Gaussian) oluşturulmuştur. Stokastik kontrol yaklaşımları, deterministik yaklaşımlar (doğrusal karesel regülatör) kadar beklenen performansı gösteremeyen mekanizmalardır. Sulama kanallarında kullanılan stokastik kontrol tekniğinin gerekli performansı gösterebilmesi için çevrim kazancı methodu uygulanarak performans ayarlaması yapılabilir. Bu tekniğin uygulanması sonucu stokastik kontrol mekanizmasında oluşan performans değişimleri frekans cevabı yöntemlerinden olan Bode diagramı ve tekil değer yöntemleri ile analiz edilmiştir. Geri beslemeli sulama kanallarının performans analizlerinde frekans cevabı yöntemlerinin sulama kanallarının işletilmesi konusunda önemli bilgiler verdiği ve stokastik kontrol mekanizmasının performansı ile ilgili yararlı veriler sağladığı görülmüştür.

Anahtar Kelimeler: geribeslemeli kontrol, sulama kanalları, tekil değerler, Bode diyagramı.

INTRODUCTION

The mounting pressure on available water supplies is resulting in a need to increase productivity of water for irrigation. With increasing demands for water for domestic use, industry and the environment supplies of water for irrigation can be expected to fall, hence the need for “more from less” in irrigated

agriculture. Better control and distribution of irrigation water within a canal network results in increased agricultural performance by providing water in a more adequate, timely and reliable manner to suit the needs and expectation of the farming community. The goal of canal operations is to match the actual flow in the canals to the required flow for that day while maintaining water surface elevations within allowable

¹ Adnan Menderes Üniversitesi Ziraat Fakültesi, Tarımsal Yapılar ve Sulama Bölümü, Aydın

limits. Canal control systems must provide timely deliveries to users with little or no wastage of water and power under predicted and unknown demands. Feedback or closed-loop control strategies can be used to regulate irrigation canals to minimize the magnitude and duration of the mismatch between the supply and the demand of water. In recent years, growing awareness of the importance of delivery flexibility and distribution equity has focused attention on improving the performance of controlled canal networks. In the past, the concepts of standard full-state control theory have been applied for driving feedback control algorithms for real-time irrigation canals (Balogun *et al.* 1985; Reddy, 1995; Liu *et al.* 1995; Malaterre, 1997; Reddy and Jacquot, 1999). However, previous papers studied performance of control systems by evaluating deviations in flow depth and changes in gate opening in the canal. They did not consider the frequency response methods for the performance analysis of the controlled irrigation systems. In order to analyze the performance of controlled irrigation canals, singular values and Bode diagram frequency respond methods can be used. These techniques has been successfully used in control engineering for decades, and have proved to be indispensable when it comes to providing insight into the benefits, limitations and problems of feedback control. One important advantage of a frequency response analysis of a control system is that it provides insight into the benefits and trade-offs of feedback control (Skogestad and Postlethwaite 1996). The objectives of this study

are to present the frequency response methods in the performance analysis of feedback controlled irrigation canals and to observe improvement in the performance of the controller with applying a loop shaping technique.

MATHEMATICAL MODELING OF OPEN-CHANNEL FLOW

The Saint-Venant equations, presented below, are used to model flow in a canal:

$$\frac{\partial A}{\partial t} + \frac{\partial Q}{\partial x} = q_l \quad (1)$$

$$\frac{\partial Q}{\partial t} + \frac{\partial(Q^2/A)}{\partial x} + gA\left(\frac{\partial y}{\partial x} - S_0 + S_f\right) = 0 \quad (2)$$

in which Q = flow rate m^3/sec ; A = wetted area, m^2 ; q_l = lateral flow, m^2/sec ; y = water depth, m ; t = time, sec ; x = longitudinal direction of channel, m ; g = gravitational acceleration, m^2/sec ; S_0 = canal bottom slope (m/m); and S_f = the friction slope, m/m . Applying a finite-difference approximation and the Taylor series expansions to Equations (1) and (2), a set of linear, ordinary differential equations is obtained for the canal with control gates and turnouts (Durdu 2003):

$$A_{11}\delta Q_j^+ + A_{12}\delta z_j^+ + A_{13}\delta Q_{j+1}^+ + A_{14}\delta z_{j+1}^+ = A'_{11}\delta Q_j + A'_{12}\delta z_j + A'_{13}\delta Q_{j+1} + A'_{14}\delta z_{j+1} + C_1 \quad (3)$$

$$A_{21}\delta Q_j^+ + A_{22}\delta z_j^+ + A_{23}\delta Q_{j+1}^+ + A_{24}\delta z_{j+1}^+ = A'_{21}\delta Q_j + A'_{22}\delta z_j + A'_{23}\delta Q_{j+1} + A'_{24}\delta z_{j+1} + C_2 \quad (4)$$

where δQ_j^+ and δz_j^+ = discharge and water-level increments from time level $t+1$ at node j ; δQ_j and δz_j = discharge and water-level increments from time level t at node j ; and A_{11} , A'_{21} , ..., A_{12} , A_{22} are the coefficients of the continuity and momentum equations, respectively, computed with known values at time level t . The state of system equation at any sampling interval k can be written, in a compact form as follows:

$$A_L \delta x(k+1) = A_R \delta x(k) + B \delta u(k) + C \delta q(k) \quad (5)$$

where $A = l \times l$ system feedback matrix, $B = l \times m$ control distribution matrix, $C = p \times l$ disturbance matrix, $\delta x(k) = l \times l$ state vector, $\delta u(k) = m \times l$ control vector, $\Delta \delta q$ = variation in demands (or disturbances) at the turnouts, m^2/s , l = number of dependent (state) variables in the system, m = number of controls (gates) in the canal, p = number of outlets in the canal, and k = time increment, sec . The elements of the matrices A , B , and C depend upon the initial condition. The dimensions of the control distribution matrix, B , depend on the number of state variables and the number of gates in the canal (Durdu 2004). The dimensions of the disturbance matrix, C , depend on the number of disturbances acting on the canal system and the number of dependent state variables. The Eq.

(5) can be written in a state-variable form along with the output equations as follows (Reddy 1999):

$$\delta x(k+1) = \Phi \delta x(k) + \Gamma \delta u(k) + \Psi \delta q(k) \quad (6)$$

$$\delta y(k) = H \delta x(k) \quad (7)$$

where $\Phi = (A_L)^{-1} * A_R$, $\Gamma = (A_L)^{-1} * B$, and $\Psi = (A_L)^{-1} * C$, $\delta y(k) = r \times 1$ vector of output (measured variables), $H = r \times l$ output matrix, and $r =$ number of outputs.

LINEAR QUADRATIC GAUSSIAN CONTROLLER (LQG)

Linear Quadratic Gaussian control theory integrates the states estimation and the controller design into a single body of knowledge. A LQG controller consists of an optimal state feedback (LQR) and an optimal state estimator (Kalman filter). LQR control problem as an optimization problem in which the cost function, J , to be minimized is given as follows (Reddy, 1999):

$$J = \sum_{i=1}^{K_{\infty}} [\delta x^T(k) Q_{x_{lxl}} \delta x(k) + \delta u^T(k) R_{mxm} \delta u(k)] \quad (8)$$

subject to the constraint that:

$$-\delta x(k+1) + \Phi \delta x(k) + \Gamma \delta u(k) = 0 \quad k = 0, \dots, K_{\infty} \quad (9)$$

where $K_{\infty} =$ number of sampling intervals considered to derive the steady state controller; $Q_{x_{lxl}} =$ state cost weighting matrix; and $R_{mxm} =$ control cost weighting

$$\delta \hat{x}(k+l) = \phi \delta \hat{x}(k) + \Gamma \delta u(k) + L[\delta y(k) - H \delta \hat{x}(k)] \quad (12)$$

in which $\delta \hat{x}(k) =$ estimated values of the state variables; and $L =$ observer gain matrix.

After calculation of optimal regulator and Kalman filter separately, both optimal regulator and Kalman filter are combined into an optimal LQG regulator, which generates the input vector, $\delta u(k)$, based upon the estimated state-vector, $\delta \hat{x}(k)$, rather than the actual state-vector, $\delta x(k)$ and the measured output vector, $\delta y(k)$.

matrix. Equations (8) and (9) constitute a constrained-minimization problem that can be solved using the method of Lagrange multipliers. In the optimal steady-state case, the solution for change in gate opening, $\delta u(k)$, is of the same form as (Reddy 1999):

$$\delta u(k) = -K \delta x(k) \quad (10)$$

Since it is expensive to measure all the state variables (flow rates and flow depths) in a canal system, the number of measurements per pool must be kept to an absolute minimum. Usually the flow depths at the upstream and downstream ends of each pool are measured (Reddy 1999). The relationship between the state variables and the measured (or output) variables is:

$$\delta y(k) = H \delta x(k) + \eta(k) \quad (11)$$

in which $\delta y(k) = N_{mo} \times 1$ vector of output variables; $H = N_{mo} \times l$ output matrix; $\eta(k) = N_{mo} \times 1$ vector of random measurement noises; and $N_{mo} =$ number of measured outputs. If the initial conditions and the inputs (control inputs and the disturbances) are known without error, the system dynamic equation (2) can be used to estimate the state variables that are not measured. Since part of the disturbances are random and usually are not measured, the canal parameters are not known very accurately, the estimated values of the state variables would diverge from the actual values. This divergence can be minimized by utilizing the difference between measured output and the estimated output (error signal), and by constantly correcting the system model with the error signal. Therefore, the modified state equations are given as (Reddy 1995):

FREQUENCY RESPONSE METHODS FOR PERFORMANCE ANALYSIS

A LQG controlled system does not have guaranteed stability margins. When a full-state feedback controller (LQR) is implemented via an observer (Kalman) based measurement feedback, the impressive properties of LQR are generally lacking. Since the closed-loop eigenvalues of the compensated (LQG) system are the eigenvalues of the regulator and the eigenvalues of the Kalman filter, if we wish to

achieve the same performance in the compensated system as the full-state feedback system (LQR), ideally we must select a Kalman filter such that the Kalman filter eigenvalues do not dominate the closed loop system, i.e. they should not be closer to the imaginary axis than the regulator eigenvalues. Since full-state feedback has great performance utilities, LQR controller is the target loop to reach the full-state feedback performance. A Feedback controlled system consists of a feedback controller (LQG) with transfer

matrix, $H(z)$, a canal system with transfer matrix, $G(z)$, with desired input $Y_d(z)$ with desired output, $Y(z)$ and disturbances, $\delta q(k)$ (Figure 1). The performance of a feedback control system is related to the return ratio matrix $G(z)H(z)$ [i.e. $H(zI - \Phi)^{-1} \Gamma$] for full state feedback and return ratio matrix $G(z)H(z)$ [i.e. $H(zI - \Phi)^{-1} \Gamma(-K(zI - \Phi + \Gamma K + LH)^{-1} K)$] for LQG. The return ratio matrix of LQG is represented by M , the norm matrix as follows (Durdu 2003):

$$\text{Norm Matrix } (M) = H(zI - \Phi)^{-1} \Gamma(-K(zI - \Phi + \Gamma K + LH)^{-1} K) \quad (13)$$

To analyze and improve the performance of a feedback controlled irrigation canal, singular values (SV) and Bode diagram techniques are used in this study.

Singular Values (SV)

The singular values help us analyze the properties of a multivariable feedback system in a manner quite similar to a single-input, single-output feedback system (Tewari 2002). For analyzing performance of control systems, we can treat the largest and smallest singular values of a return difference (or return ratio) matrix as providing the upper and lower bounds on the scalar return difference (or return ratio) of an equivalent single-loop system. For example if system transfer matrix is $G(z)$ and feedback controller matrix $H(z)$, then to maximize performance of the system, we should minimize the singular values of the sensitivity matrix, $[I + G(z)H(z)]^{-1}$ which implies minimizing the largest singular value, $\sigma_{max}[I +$

$G(z)H(z)]^{-1}$, or maximizing the singular values of the return difference matrix at the output, i.e. maximizing $\sigma_{min}[I + G(z)H(z)]$. The singular values of the return difference matrix at the output in the frequency domain $\sigma[I + G(i\omega)H(i\omega)]$, can be used to estimate the gain and phase margins of a multivariable system (Tewari 2002). The way in which multivariable gain and phase margins are defined with respect to the singular values is as follows: take the smallest singular value, σ_{min} , of all the singular values of the return difference matrix at the output, and find a real constant, a , such that $\sigma_{min}[I + G(i\omega)] \geq a$ for all frequencies, ω , in the frequency range of interest. Then the gain and phase margins can be defined as follows (Tewari 2002):

$$\text{Gain Margin} = 1/(1 \pm a) \quad (14)$$

$$\text{Phase Margin} = \pm 2\sin^{-1}(a/2) \quad (15)$$

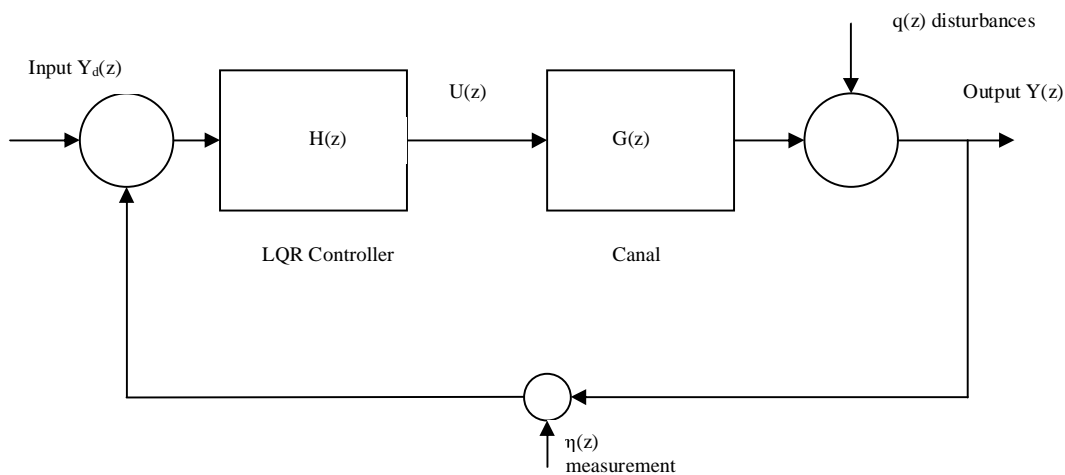


Figure 1. A Feedback control system scheme.

The adjustment of the singular values of return ratio matrices to achieve desired closed-loop performance is called loop shaping. This term derived from single-loop systems where scalar return ratios of a loop are to be adjusted. For compensated systems based on an observer (i.e. the Kalman filter), generally there is a loss of performance, when compared to full-state feedback control systems. To recover the performance properties associated with full-state feedback, the Kalman filter must be designed such that the sensitivity of the system's input to process and measurement error is minimized. This requires that the smallest singular value of the return ratio at plant's input, $\sigma_{min}[H(z)G(z)]$, should be maximized. Theoretically, this maximum value of $\sigma_{min}[H(z)G(z)]$ should be equal to that of the return ratio at the plant's input with full-state feedback (Tewari 2002).

Bode Diagram

Bode diagram contains two plots in rectangular coordinates, in which the magnitude is expressed in decibels (dB), and the phase angle in degrees, both

plotted as functions of the logarithm of frequency in rad/unit time (normally, rad s⁻¹). Bode diagrams are normally plotted on semi-logarithmic graph paper, so that the dB values plotted on the linear vertical axis have the effect of producing a logarithmic scale, while the frequency values can be plotted directly on the horizontal axis, allowing the logarithmic axis to do the work of conversion. The frequency response magnitude ratio is expressed in decibels using (Tewari 2002) :

$$M(\omega)_{dB} = 20 \log_{10} M(\omega) \quad (16)$$

where $M(\omega)_{dB}$ is the log modulus in decibels and $M(\omega)$ is the magnitude ratio. Typical Bode plots are shown in Figure 2. For convenience, the two types of diagram are shown together. For a control system having desired input $Y_d(z)$ and output $Y(z)$, the transfer function model is defined as the z transformed output $Y(z)$ divided by input $Y_d(z)$, such that:

$$Y(z)/Y_d(z) = G(z)H(z)/[1+G(z)H(z)] = F(z) \quad (17)$$

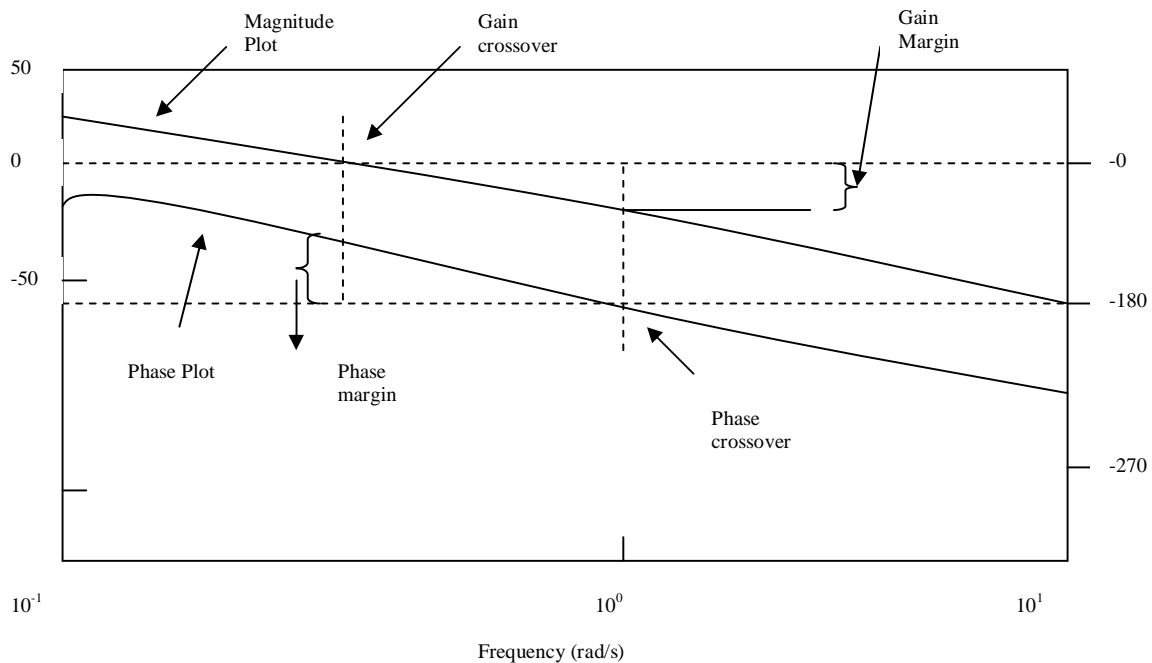


Figure 2. Singular values of LQG controlled open-channel.

Consider the Bode form of a transfer function $F(z)$ for which the frequency response is (Tewari 2002):

$$F(j\omega) = K_B \prod_{i=1}^m [1 + j(\omega/z_i)] / (j\omega)^r \prod_{i=1}^{n-r} [1 + j(\omega/p_i)] \quad (18)$$

where K_B is Bode gain, m and n are the numbers of terms in the numerator and denominator, respectively, z_i and p_i are the non-zero finite zeros and poles respectively of $F(z)$, r is system type. A constant K_B provides a magnitude contribution of $20 \log_{10} |K_B|$ and a phase angle of 0° if K_B is positive, or -180° if K_B is negative. If $K_B = 1$, then $20 \log_{10} |K_B|$ is zero dB; if $K_B = 2$, then the dB magnitude is 6 and if $K_B = 0.5$, the dB magnitude is -6. In all three cases the phase angle contribution is 0° . For $K_B = -2$ or -0.5 , the dB magnitude would be 6 or -6, respectively, but the phase contribution would be -180° .

RESULTS AND ANALYSIS

To demonstrate the effectiveness of frequency response methods in the performance analysis of feedback controlled irrigation canals, an LQG regulation problem for a discrete-time multi-pool irrigation canal had been simulated. The data used was as follows: length of canal reach = 52500 m, number of nodes = 49, number of sub-reaches used = 6, $\Delta x = 1500$ m, channel slope = 0.0002, side slope = 1.0, bottom width = 5 m, disturbance along the simulation = $2.5 \text{ m}^3/\text{s}$, discharge required at the end of the canal = $5 \text{ m}^3/\text{s}$, target depth at downstream end = 1.5 m, gate width = 5 m, and gate discharge coefficient = 0.8. First this data was used to calculate the steady state values, which in turn were used to compute the initial gate openings and the elements of the Φ , Γ , H matrices using sampling interval of 30 sec. The values of the initial gate openings for gate1, gate2, gate3, gate4, gate5, gate 6 and gate 7 were 1.1338 m, 1.368 m, 1.1686 m, 0.9782 m, 0.8583 m, 0.6372 m and 0.7055 m, respectively. At first part of LQG controller, a Linear Quadratic controller was designed to regulate the six pool canal system using a constant-level control approach. The system response was simulated using the controller in the feedback loop. In the derivation of the feedback gain matrix K , the control cost weighting matrix, R , of dimensions 12, was set equal to 100, whereas the state cost weighting matrix, Qx , was set equal to an identity matrix of dimensions 85. The matrix dimension 85 comes from the system dimension. Since the irrigation canal is divided into 49 nodes and each node has a set of two equations, in other words the dimension of the system should have

been 98. But the system has 7 gates and 6 turnouts; therefore, the system matrix dimensions were 85. The cost weighting matrix and the control cost matrix must be symmetric and positive definite (i.e. all eigenvalues of R and Qx must be positive real numbers). A priori, we do not quite know what values of Qx and R will produce the desired effect. In the absence of a well-defined procedure for selecting the elements of these matrices, these values were selected based upon trial and error. At first, we began by selecting both Qx and R as identity matrices. By doing so, we were specifying that all state variables and control inputs were equally important in the objective function, i.e. it was equally important to bring all the deviations in the state variables (water surface elevations and flow rate) and the deviations in the control inputs to zero while minimizing their overshoots. Note that the existence of a unique, positive definite solution to the algebraic Riccati equation (Eq. 19) is guaranteed if Qx and R are positive semi-definite and positive definite, respectively, and the system is controllable. After defining Qx and R matrices, the optimal feedback gain matrix, K , was calculated. A Kalman filter technique was used to estimate the values for the state variables in the system. Kalman filter for the system used the control input $\delta u(k)$, generated by the LQR, measured water depths $\delta y(k)$ for each pool, and the disturbances $\delta q(k)$ and $\eta(k)$ with known power spectral densities, ρ . In the design of the Kalman filter, in lieu of actual field data on withdrawal rates from the turnouts, the random disturbances were assumed to have some prespecified levels of variance. The variances of the disturbances must be estimated from historical records on water withdrawals from the canal outlets. The variances of the disturbances were: $w_1 = 1^2$, $w_2 = 1.3^2$, $w_3 = 0.7^2$, $w_4 = 1.4^2$ and $w_5 = 1.3^2$. A value of 0.0005 was used for the variance of the measurement spectral density matrix (RC), and it was an identity matrix. Using the given initial values, the system response was simulated for 250 time increments or 7500 seconds. The analysis was started by evaluating the system stability. All the eigenvalues of the feedback matrix were positive and had values less than one. In the derivation of the control matrix elements, Γ , it was assumed that both the upstream and downstream gates of each reach could be manipulated to control the system dynamics. The downstream-end gate (gate 7)

position was frozen at the original steady state value, and only the upstream-end gate (gate 1) of the given reach was controlled to maintain the system at the equilibrium condition. The effect of variations in the opening of the downstream gate must be taken into account through real-time feedback of the actual depths immediately upstream and downstream of the downstream gate (node N). The frequency range, ω , was chosen between 10^{-6} and 10^2 .

For performance analysis of the feedback controlled irrigation canal, the frequency response methods were used to show the system's response to the initial conditions at different frequency ranges, ω (bandwidth). Singular values (SV) and Bode plot diagrams were conducted for the system. LQR controlled system had a gain margin equal to infinity for each control input of the system. Since LQR controller had the best performance properties, the performance analysis of the LQG controller used the LQR performance properties as a target. As shown in Figure 3, for the sake of simplicity, the maximum singular values of the LQG and the LQR controller are not shown. Figure 3 illustrates that there are some differences between the minimum singular values of the LQG compensated system and the full-state feedback system. The y-axes of Figure 3 represent the magnitude of the singular values of the return ratio matrix in decibel and the x-axes of Figure 3 represent the frequency of the disturbances. For LQR controller, the return ratio, $G(z)H(z)$, is equal to $-K(zI-\Phi)^{-1}\Gamma$.

When the LQG compensated controller was designed, the singular values of the return ratio, $G(z)H(z)$, was targeted to approach the corresponding singular values of the LQR controller. To determine the stability of the LQG and the LQR controllers, it was monitored that if the singular values of the return ratio were close to zero. Since the LQR was the target loop function, the investigation concentrated on adjusting the LQG's singular value curves as close as to the possible LQR's singular value curves. It was obvious from Figure 3 that the all 5 pools were stable at higher sinusoidal frequencies for LQR controller but when the frequency was 0.1 rad/sec, the oscillatory behavior in the canal occurred. At all 5 pools the singular values of LQG controller were far away from zero in comparison to LQR singular values. When the sinusoidal frequency, ω , increased, all pools started having higher oscillations. But as far as the performance of LQG was concerned, the system had less performance than LQR did. It was obvious that if LQR and Kalman filter were combined together, there will be a loss of performance for the new compensated controller (LQG) in comparison to the full-state feedback LQR controller. To recover the full-state feedback performance in LQG controller, Kalman filter spectral density matrix was readjusted by using a loop shaping technique. As demonstrated in Figure 3, the singular values of LQG controller were approaching the LQR singular values. In other words, LQG controller

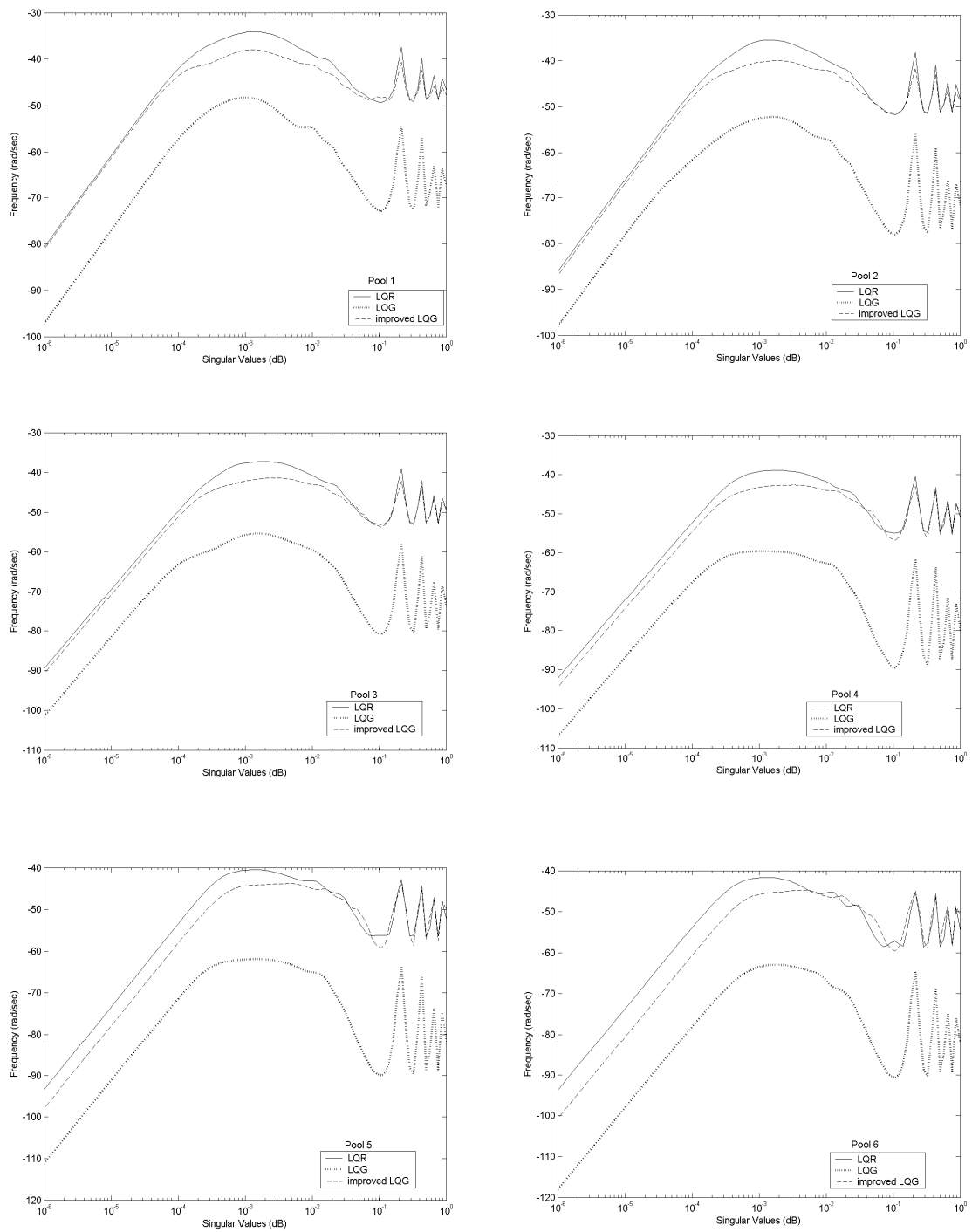


Figure 3. Stability margins on Bode diagram.

performance was improved by using a loop shaping technique. Pool 1, 2, 3, and 4 had relatively good recovery of LQR performance. Singular values of LQG in pool 5 and 6 came closer to LQR's singular values but not as much as the other pools did. Also oscillations of LQG's singular values started at 0.1 rad/sec. At lower sinusoidal frequencies LQG controller was stable.

Bode plot is the other option to investigate the performance analysis of the feedback controller systems. Figure 4 illustrates gain and phase margin diagrams for all the irrigation canal pools. A 12-set of Bode diagram for each pool was obtained. The reason for that the system had 12 external inputs (disturbance), two for each pool (one at the beginning of the sampling interval and the other at the end of the sampling interval). From these graphs it was obvious that the LQG controller did not have a good performance like LQR did. As shown in Figure 5, the gain margin for both LQG and the LQR controller was high and the curves were far away from 0 dB. If the curves were close to or over the 0 dB, the system would be unstable and the gain margin would be small. Gain diagram illustrated that LQG and LQR controllers were both stable but the phase diagram did not allow one to make that same statement about the performance of the LQG controller. It was obvious that LQR curves in all pools had a cross over with -180 degrees around a disturbance frequency of 0.105 rad/sec and it had a large frequency range (bandwidth) for stability. A comparison of the LQR and the LQG stability bandwidths reveals that LQR is stable at all disturbance frequencies whereas LQG has less frequency range for stability. In Pool 1, the LQG curve did not have a phase crossover with -180 degrees. In other words, LQG controller did not have a good performance in pool 1 but with applying loop shaping technique the curve in the phase diagram moved upward and it had a crossover with -180 degrees at a frequency of 0.000407 rad/sec.

Frequencies more than this value caused loss of performance in the pool 1. LQG phase curve did not have a crossover in pool 2 but loop shaping moved LQG's phase curve towards LQR's curve and the phase curve had a crossover with -180 degrees at a frequency of 0.000667 rad/sec. In pool 3, both LQG and improved LQG phase curves had a crossover with -180 degrees at a frequency of the 0.000558 rad/sec. LQG controller did not present a good performance at low frequencies but applying loop shaping technique helped LQG phase curve move upward and improve its performance. In pool 4, both LQG and improved LQG phase curves had a crossover at a frequency of the 0.000656 rad/sec. At low frequencies LQG controller did not show a good performance but loop shaping improved LQG performance at low frequencies too. If the frequency range of the disturbance was increased beyond 0.000656 rad/sec, there would be loss of stability in pool 4. Like in pool 3 and 4, in pool 5, LQG controller did not have a good performance at low frequencies. The crossover with -180 degrees occurred at a frequency of 0.000646 rad/sec. A frequency range more then this value caused loss of performance in the pool 5. LQG phase curve presents that pool 6 did not have a good performance along the simulation and there was no crossover with -180 degrees. With loop shaping technique, LQG controller's phase curve moved towards LQR phase curve and had a crossover at a frequency of 0.00141 rad/sec. But there was a loss of performance at a low frequency bandwidth where the frequency range was between 2.19×10^{-10} and 5.17×10^{-10} . It can be observed that phase diagrams of pool 1, pool 2 and pool 6 had significant differences between LQG and LQR phase curves. The reason for that in pool 1 and pool 2, there was an increase in the opening of the upstream gate and release more water to compensate for the demands at downstream end. In pool 6, the differences in phase curves were because of meeting target depth at downstream end.

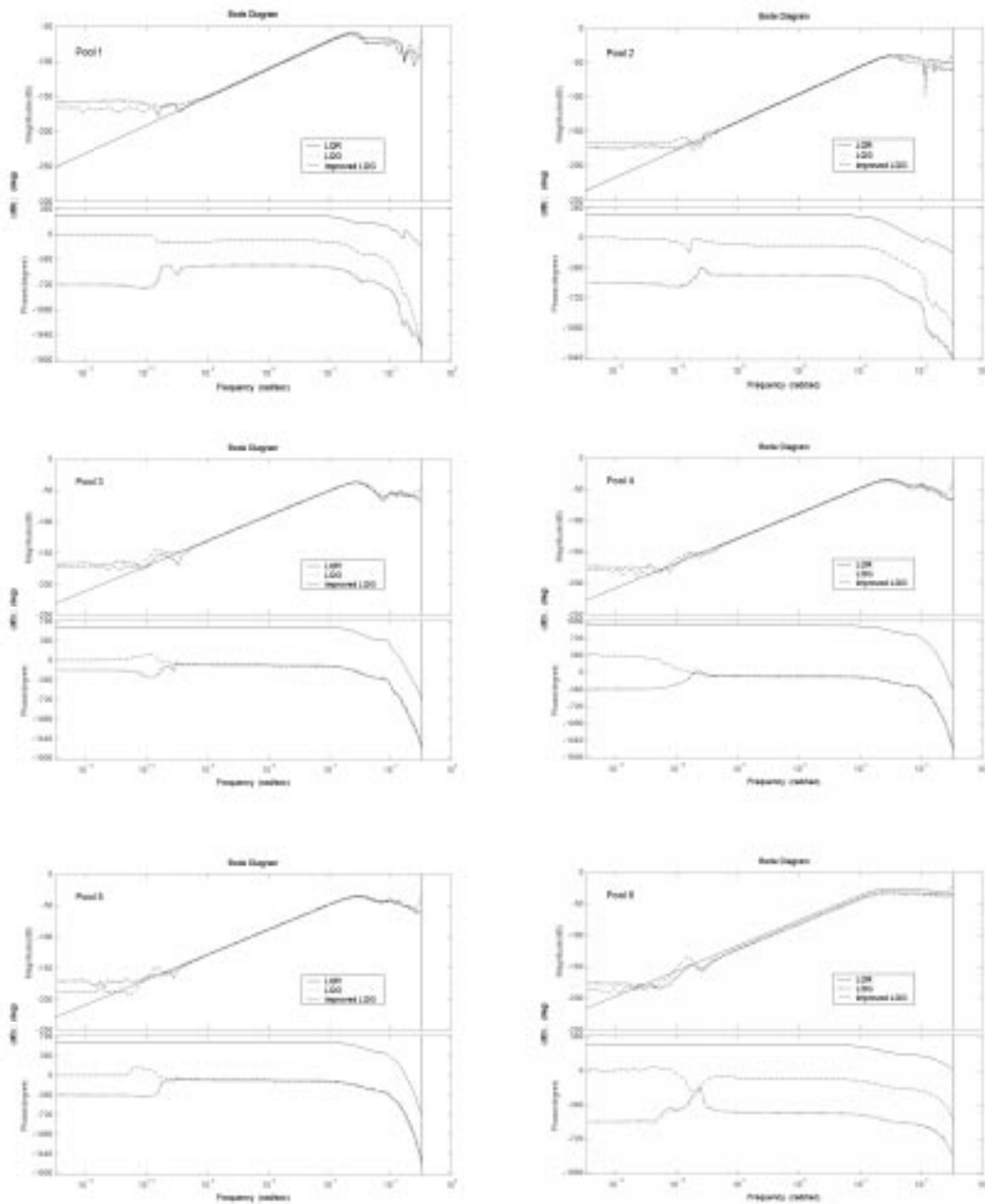


Figure 4. Bode diagrams of LQG controlled open-channel

Figure 5 illustrates the variations in flow depth in all pools for LQR, LQG and improved LQG. It was obvious that LQR controller had more

variations in flow depth than LQG and improved LQG. Because of robustness and stability properties of the LQR, LQR variations curves must be chosen as

target loops. As mentioned above first and last pools had highest flow depth variations among the other pools. The decrease in the downstream depth of flow resulted in a sudden increase in gate opening (0.6 m) at the upstream end of the reach to release more water into the canal. However, because of the wave travel time, the depth of flow at the downstream end did not start to rise until 3000 s. With applying loop shaping technique flow depth variations curves in all pools moved towards LQR curves.

CONCLUSIONS

The purpose of this study has been show that Bode diagram and singular values methods can be applied in the performance analysis of feedback controlled open-channel with multiple gates and pools. To design a feedback control system, the basic nonlinear hydrodynamic partial equations for open-channel flow were discretized and linearized about equilibrium conditions. The feedback control theory augmented with loop shaping is a very powerful design synthesis procedure to improve the performance of the system. To demonstrate their effectiveness, Bode diagram and singular values techniques were applied to a feedback controlled irrigation canal with 6 pools and 7 gates. At first Linear Quadratic Regulator (LQR) was applied to the canal system using a constant-level approach and the results were observed. It was assumed that all the state variables (flow rate and flow depth) were available in

the designing of LQR. Therefore LQR control has good stability margins. Since it was expensive to measure all the flow depth and flow rates along the canal, a Kalman estimator was designed to estimate the state variables at unmeasured nodes. Combining LQR and Kalman estimator resulted in a LQG control system for the open-channel. However, for a LQG controlled system, there are no guaranteed stability margins. Therefore, Bode diagram and singular values techniques were applied to feedback controlled irrigation canal to analyze the performance of the system. The results from gain graphs of Bode diagram demonstrated that LQR curves at all pools was under 0 dB. Also results from phase graphs showed that LQR curves had a crossover with -180 degrees at all pools. This implies that LQR curves had great performance in the operation of canal control. At first, phase curves of LQG controller demonstrated that LQG feedback controlled system did not have good performance but with applying loop shaping technique LQG's performance reached to LQR's performance in the control of the canal. Overall the results of this study show that Bode diagram and singular value methods are acceptable techniques in the performance analysis of feedback controlled irrigation canals. Also these methods have a great illustration capability to show the improvement in the performance of controlled canals via a loop shaping technique.

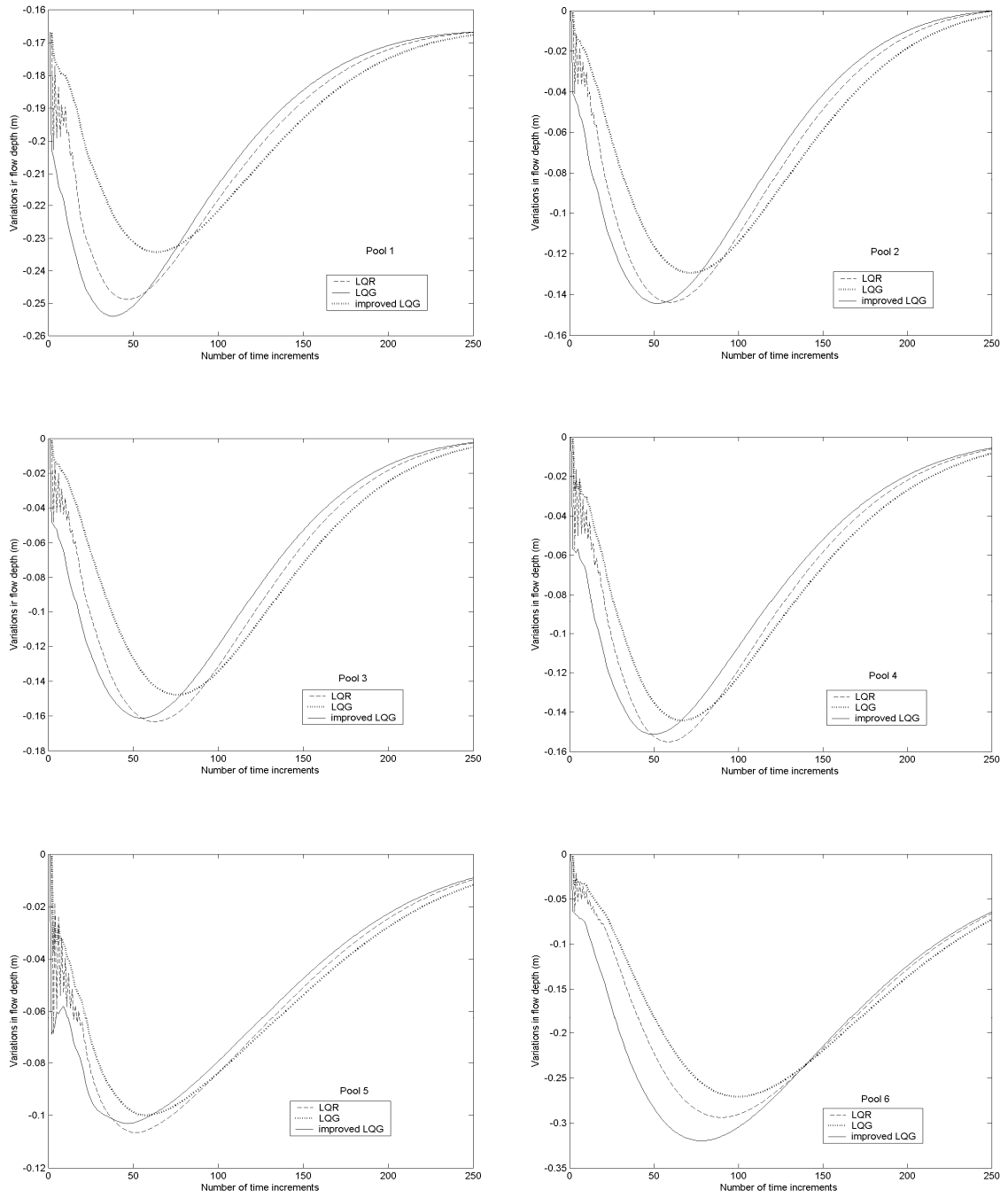


Figure 5. Variations in flow depth at each pool.

REFERENCES

- Balogun, O.S., 1985. Design of Real-time Feedback Control for Canal Systems using Linear Quadratic Regulator Theory, Ph.D dissertation, Department of Mechanical Engineering, University of California at Davis, USA.
- Durdu, O.F., 2003, Robust Control of Irrigation Canals, Ph.D. dissertation, Colorado State University, Civil Engineering Department, Fort Collins, CO, USA.
- Durdu, O.F., 2004. Optimal Control of Irrigation Canals using Recurrent Dynamic Neural Networks (RDNN), Proceedings of the ASCE EWRI 2004 World Water & Environmental Resources Congress, June 27-July 1, 2004, Salt Lake City, UT: ASCE, CD-rom, 14 pp.
- Liu, F., Berlamont, J., Feyen, J., 1995. Downstream Control of Multireach Canal Systems, Journal of Irrigation and Drainage Engineering, ASCE, 121(2), 179-190.
- Malaterre, P.O., 1997. Multivariable Predictive Control of Irrigation Canals. Design and Evaluation on an a 2-pool Model, International Workshop on Regulation of Irrigation Canals, 230-238, Morocco, 1997.
- Reddy, J.M., 1995. Kalman Filtering in the Control of Irrigation Canals, Int. J. Appl. Math. Modeling, 19(4), 201-209.
- Reddy, J.M., 1999. Simulation of Feedback Controlled Irrigation Canals, Proceedings USCID Workshop, Modernization of Irrigation Water Delivery Systems, 605-617.
- Reddy, J.M., Jacquot, R.G., 1999. Stochastic Optimal and Suboptimal Control of Irrigation Canals, J. of Water Resources Pln. and Mgt., 125, 369-378.
- Skogestad, S., Postlethwaite, I., 1996. Multivariable Feedback Control. Wiley, New York.
- Tewari, A., 2002. Modern Control Design with Matlab and Simulink, Wiley, New York.

Geliş Tarihi : 23.01.2009

Kabul Tarihi : 27.03.2009

